

Kinesin Spindle Protein Inhibitors with Diaryl Amine Scaffolds: Crystal Packing Analysis for Improved Aqueous Solubility

Tomoki Takeuchi,[†] Shinya Oishi,^{*,†} Masato Kaneda,[†] Hiroaki Ohno,[†] Shinya Nakamura,[‡] Isao Nakanishi,[‡] Masayoshi Yamane,[§] Jun-ichi Sawada,[§] Akira Asai,[§] and Nobutaka Fujii^{*,†}

[†]Graduate School of Pharmaceutical Sciences, Kyoto University, Sakyo-ku, Kyoto 606-8501, Japan

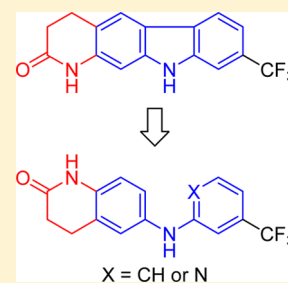
[‡]Faculty of Pharmacy, Kinki University, 3-4-1 Kowakae, Higashi-osaka 577-8502, Japan

[§]Graduate School of Pharmaceutical Sciences, University of Shizuoka, Suruga-ku, Shizuoka 422-8526, Japan

Supporting Information

ABSTRACT: Diaryl amine derivatives have been designed and synthesized as novel kinesin spindle protein (KSP) inhibitors based on planar carbazole-type KSP inhibitors with poor aqueous solubility. The new generation of inhibitors was found to show comparable inhibitory activity and high selectivity for KSP, and this was accompanied with improved solubility. Kinetic analysis and molecular modeling studies suggested that these inhibitors work in an ATP-competitive manner via binding to the secondary allosteric site formed by $\alpha 4$ and $\alpha 6$ helices of KSP. Comparative structural investigations on a series of compounds revealed that the higher solubility of diaryl amine-type inhibitors was attributed to fewer van der Waals interactions in the crystal packing and the hydrogen-bond acceptor nitrogen of the aniline moiety for favorable solvation.

KEYWORDS: Aqueous solubility, crystal packing, diphenylamine, kinesin spindle protein



The kinesin spindle protein (KSP; also known as Eg5) is a member of the kinesin superfamily of molecular motor proteins.¹ The KSP moves toward the plus end of microtubules using the energy generated from ATP hydrolysis. This KSP movement produces the outward force that pushes the centrosomes apart during cell division and provides the following formation of the bipolar spindle. Inhibition of KSP prevents spindle pole separation, which leads to prolonged mitotic arrest in prometaphase and subsequent apoptosis.² Unlike tubulin and microtubules, KSP expression is abundant only in dividing cells, but not in postmitotic neurons in the human central nervous system.³ Therefore, KSP inhibitors are expected to be more favorable agents for cancer chemotherapy without the neurotoxic side effects seen with traditional antimetabolic agents (e.g., taxanes and vinca alkaloids).^{4–6} To date, several clinical trials of potent KSP inhibitors including ispinesib, SB-743921, AZD4877, ARRY-520, and 4SC-205 have been conducted.¹

Recently, we reported that carbazole derivative **3** exhibited potent KSP inhibitory activity.⁷ On the basis of the common substructure of the known KSP inhibitory terpendole **1** and HR22C16 **2** (Figure 1),^{8,9} the ring-fused indoles were identified to be minimal scaffolds for KSP inhibition. Further structure–activity relationship studies from carbazole **3** in combination with the known biphenyl-type KSP inhibitors like **4**^{10–12} revealed that a carboline **5** and a lactam-fused carbazole **6a** exhibited potent KSP ATPase inhibitory activity and cytotoxicity via effective cell-cycle arrest at the M-phase.¹³ During the course of our investigations on antitumor effects of these carbazole-based KSP inhibitors,^{14,15} we found that these inhibitors exhibited limited solubility in aqueous solvents

employed for in vivo studies. To overcome the inherent drawbacks of carbazole-based KSP inhibitors, we undertook research on the development of novel diaryl amine-type KSP inhibitors to simultaneously satisfy the potent inhibitory activity as well as show much better solubility in aqueous solution. The structural basis of the solubility of a series of compounds was also investigated by single-crystal X-ray diffraction studies and free energy calculations.

The melting points of carbazole-type KSP inhibitors **6a,b** were extremely high (Figure 1). We speculated that the poor solubility of compound **6** would be attributable to the significant intermolecular interactions in the crystals since the melting point is correlated with the crystal packing of the molecule, which is one of the major contributing factors to solubility.¹⁶ With the aim of disrupting the possible intermolecular π – π stacking interactions to lower the melting point and in turn to improve the solubility, the design of more nonplanar analogues from planar compounds **6** was expected to be a promising approach.¹⁶ Alternatively, the addition of polar or ionizable functional group(s) is also an effective modification to enhance solubility. To satisfy these two criteria, we designed diphenylamine derivatives **7a,b**, in which the pyrrole C–C bond in the central part of carbazoles **6a,b** was cleaved (Figure 1). It was expected that the two aryl rings in potentially noncoplanar conformations in **7** would prevent intermolecular π – π stacking interactions and that the newly available aniline would enhance solubility in an aqueous environment.

Received: January 16, 2014

Accepted: March 10, 2014

Published: March 10, 2014

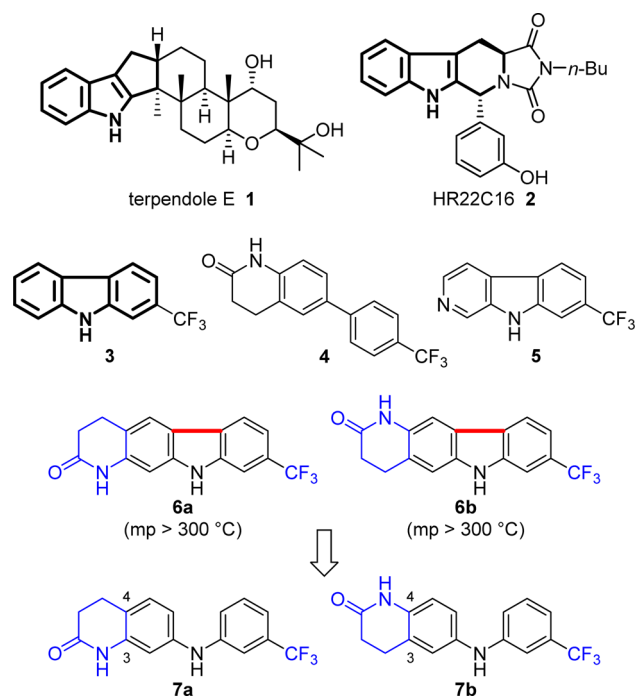


Figure 1. Structures of the reported KSP inhibitors 1–6 and design of novel KSP inhibitors 7 with a diphenylamine scaffold.

A series of diaryl amine derivatives 7 and 8 were prepared by palladium-catalyzed *N*-arylation using aryl bromides and substituted anilines (see Supporting Information).¹⁷ The diphenylamine derivatives 7a,b were initially evaluated for KSP ATPase inhibitory activity (Table 1). Diphenylamine 7a with the accessory amide group at the 3-position on the left-hand phenyl group showed no KSP inhibitory activity; although the parent carbazole 6a showed highly potent activity. However, diphenylamine 7b with the amide group at the 4-

Table 1. KSP Inhibitory Activities of Diphenylamines with a 3,4-Fused Lactam Structure on the Left-Hand Phenyl Group and the Related Carbazoles

compound	KSP ATPase IC ₅₀ (μM) ^{a,b}
	6a 0.031
	6b 0.18
	7a >6.3
	7b 0.045

^aInhibition of microtubule-activated KSP ATPase activity. ^bIC₅₀ values were derived from the dose–response curves generated from triplicate data points.

position exhibited four times more potency (IC₅₀ = 0.045 μM) than the parent carbazole 6b. This potency was comparable to that of the most potent carbazole-type inhibitor 6a. Diphenylamine 7b showed a good inhibitory effect on the proliferation of cancer cell lines: A549, HCT-116, and MCF-7 (see Supporting Information).

To investigate the selectivity of diphenylamine 7b, inhibitory activities were evaluated for a number of the other kinesins. The ATPase activities of centromere-associated protein E (CENP-E), Kid, mitotic kinesin-like protein 1 (MKLP-1), KIF4A, KIFC3, KIF14, and KIF2A were not inhibited by 7b at 20 μM (see Supporting Information), which is consistent with the selectivity profile of carbazole-type inhibitor 6a. The diphenylamine 7b was also screened in comparison with β-carboline 5 and carbazole 6a against a panel of 117 kinases to assess the selectivity profiles (see Supporting Information). β-Carboline 5 showed >50% inhibition against four kinases (CDK6/cyclinD3, IKKβ, PRK2, and ROCK-II) at 10 μM, which is consistent with previous studies showing that carboline is a well-known scaffold of kinase inhibitors.¹⁸ However, no more than 50% inhibition against any kinases was observed in 6a and 7b (10 μM), suggesting that newly identified diphenylamine-type inhibitor 7b has high selectivity for KSP.

To estimate the possible binding pocket of the diaryl amine-type inhibitor 7b, kinetic experiments of KSP ATPase were conducted as a function of ATP concentration in the absence or presence of 7b (see Supporting Information). Lineweaver–Burk plots revealed that the maximum velocity (*V*_{max}) value in the presence of 7b was identical to that in the absence of 7b. This suggested that diphenylamine 7b inhibited KSP ATPase activity in an ATP-competitive manner as observed for biphenyl 4, β-carboline 5, and carbazole 6a,¹³ possibly by binding to the ATP binding site or the α4/α6 allosteric site.¹¹

To further provide insights into the binding site of diaryl amine-type KSP inhibitors, possible interactions of diphenylamine 7b to three possible binding sites (i.e., the ATP binding site, the α2/α3/L5 allosteric site, and the α4/α6 allosteric site) were estimated by a simulated docking study using the MM/GBVI method. The predicted binding affinity (*E*_{bind}) of 7b to the α4/α6 allosteric site (−24.7 kcal/mol) was higher than the values computed to the other sites (−20.3 kcal/mol for the ATP binding site; −19.7 kcal/mol for the α2/α3/L5 allosteric site). In addition, the high selectivity of 7b for KSP compared with any other kinesins and kinases also supports the unlikely affinity to the ATP binding pocket, which is highly conserved among kinesins.¹⁹

The docking pose of diphenylamine 7b in the pocket formed by helices α4 and α6 is shown in Figure 2. Compound 7b exhibited a twisted conformation of the two aryl groups, which were buried in the pocket. The aniline NH group forms a strong hydrogen bond with the backbone carbonyl oxygen of Leu292. The 3-trifluoromethyl group interacts with a large hydrophobic pocket formed by Tyr104, Ile299, Thr300, Ile332, Tyr352, Ala353, and Ala356 through van der Waals interactions. A π–π stacking interaction between the trifluoromethylphenyl group in 7b and the Tyr104 side chain was also observed. The lactam carbonyl group in 7b forms a hydrogen bond with the side chain amide NH₂ group of Asn271. In addition, the lactam-fused phenyl group forms a π–π interaction with the Tyr352 side chain.

The solubility of a series of potent KSP inhibitors was evaluated by a thermodynamic method (Table 2).²⁰ A mixture of EtOH–phosphate buffer (pH 7.4) (1:1) [50% EtOH] was

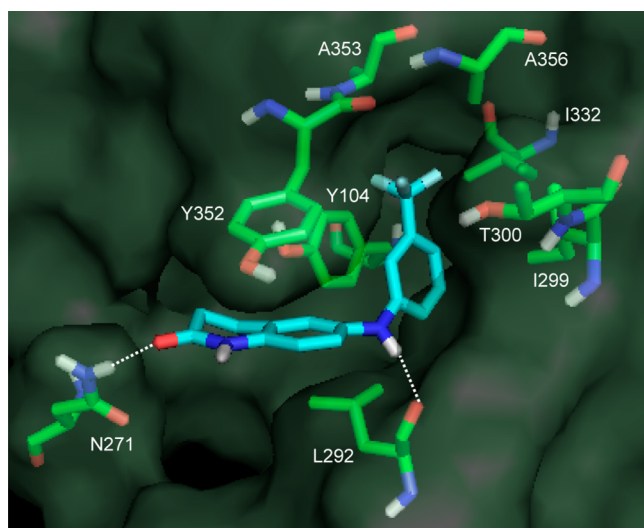


Figure 2. Docking mode of diphenylamine **7b** at the interface of helices $\alpha 4$ and $\alpha 6$.

employed as aqueous media.²⁰ In the solution, the parent carbazole-type inhibitor **3** was moderately soluble (0.424 mg/mL). Biphenyl compound **4** showed the lowest solubility in this examination (0.339 mg/mL in 50% EtOH). Carbazoles **6a,b** were slightly more soluble (0.457 mg/mL and 0.468 mg/mL, respectively, in 50% EtOH) compared with biphenyl **4**. Diphenylamine **7b** was approximately four times more soluble (1.80 mg/mL in 50% EtOH) than carbazoles **6a,b**.²¹ The physicochemical parameters such as melting point and retention time on a reversed-phase HPLC column were also investigated to estimate the underlying factors contributing to the solubility. The melting point of diphenylamine **7b** (190 °C) was significantly lower than those of biphenyl **4** (221 °C) and carbazoles **6a,b** (>300 °C). In contrast, there were no correlations between the solubility in 50% EtOH and HPLC

retention time. ClogP values of a series of compounds were similar (3.9–4.2).

The solubility of a solid inhibitor in water depends on two factors: the crystallinity of the compound and the ability of the compound to interact with water.²² Recently, trials to address solubility issues of drug candidates based on X-ray crystal structures have been reported.²³ Thus, we analyzed the crystal structures of the series of inhibitors to investigate the possible correlation with solubility (Figure 3). First, single crystals of biphenyl-type inhibitor **4** were prepared by slow evaporation of Et₂O for X-ray structural analysis. Eight equivalent biphenyl molecules **4** in a unit cell exhibited a slightly twisted conformation with a relatively small dihedral angle between the two phenyl groups (34.0°) (Figure 3A,B). Two phenyl groups of **4** are involved in a number of CH/ π interactions with the methylene groups on lactam moieties or with the phenyl groups of adjacent molecules, which would possibly contribute to large van der Waals interactions for crystal packing. The electrostatic stabilization in this packing mainly came from two intermolecular hydrogen bonds between the lactam amide groups across a pair of molecules. The packing energy of **4** calculated from the crystal structure by the MM method was –55.2 kcal/mol (vdW, –37.6 kcal/mol; electrostatic, –17.6 kcal/mol) (Table 2).

Single crystals of carbazole **6a**, which were obtained from an EtOH solution,²⁴ contained eight carbazole molecules, four EtOH molecules, and two water molecules in a unit cell (Figure 3C,D). In the packing modes of crystals, intermolecular π – π stacking interactions with the adjacent carbazoles were clearly observed (average distance between two carbazole rings: 3.81 Å). The carbazole moiety also formed CH/ π interactions with other molecules of **6a**, but the number of interactions was less when compared with that of **4**. Regarding electrostatic interactions, there were two hydrogen bonds between the lactam amide groups across a pair of molecules of **6a** as observed in the biphenyl **4** crystal. Additionally, the carbazole NH group in **6a** also interacted with an oxygen atom of EtOH or water via a hydrogen bond, leading to an increase in the

Table 2. KSP Inhibitory Activities and Physicochemical Properties of Biphenyl **4**, Carbazole **6a,b**, and Diphenylamine **7b** with a Lactam-Fused Structure

	4	6a	6b	7b
KSP ATPase IC ₅₀ (μM) ^{a,b}	0.046	0.031	0.18	0.045
solubility (mg/mL) ^{c,d}	0.339	0.457	0.468	1.80
melting point (°C)	221	>300	>300	190
crystal packing energy (kcal/mol) ^e	–55.2 (vdW: –37.6; ele: –17.6)	–58.8 (vdW: –31.8; ele: –27.0)	– ^f	–53.7 (vdW: –29.7; ele: –24.0)
ClogP ^g	4.2	3.9	3.9	4.2
HPLC retention time (min) ^h	29.0	25.9	21.7	24.4

^aInhibition of microtubule-activated KSP ATPase activity. ^bIC₅₀ values were derived from the dose–response curves generated from triplicate data points. ^cSolubility in 50% EtOH [an equal volume of EtOH and 1/15 M phosphate buffer (pH 7.4)]. ^dThe solubility in phosphate buffer (pH 7.4) of compounds **4**, **6a,b**, and **7b** was <1 μg/mL. ^eContributions of van der Waals (vdW) and electrostatic (ele) energies are shown in the brackets. ^fNot tested. ^gClogP values were calculated with ChemBioDraw Ultra 12.0. ^hHPLC analysis was carried out on a Cosmosil 5C18-ARII column (4.6 × 250 mm), and the material eluted by a linear MeCN gradient (70:30 to 30:70 over 40 min) in 0.1% TFA; flow rate of 1 mL/min.

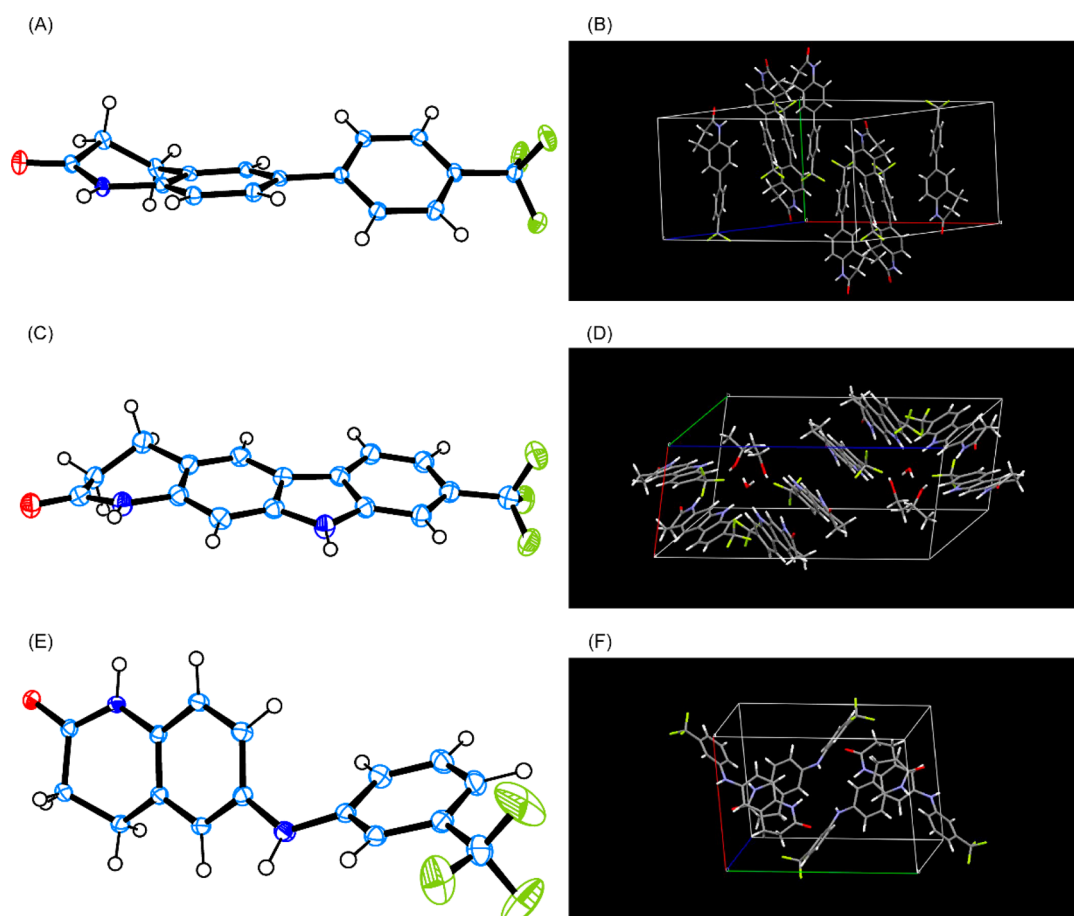


Figure 3. X-ray crystal structures of biphenyl-type (**4**), carbazole-type (**6a**), and diphenylamine-type (**7b**) KSP inhibitors. (A) ORTEP diagram; (B) crystal packing of **4**. (C) ORTEP diagram; (D) crystal packing of **6a**. (E) ORTEP diagram; (F) crystal packing of **7b**.

electrostatic interaction contribution for the total packing energy when compared with biphenyl **4**. The average value from four unique carbazole molecules in a unit cell was calculated for the packing energies of **6a** [−58.8 kcal/mol (vdW, −31.8 kcal/mol; electrostatic, −27.0 kcal/mol)] (Table 2 and Supporting Information).

Crystal structure analysis of **7b** was then performed using colorless single crystals from EtOAc in which four equivalent molecules were included in a unit cell (Figure 3E,F). No π – π interactions of the aryl groups in **7b** with the adjacent molecules were involved in the crystal packing, as we expected given that the possibly large torsion angle between the two phenyl groups in the diphenylamine **7b** would collapse the intermolecular π – π stacking of planar carbazole **6a**. Two intermolecular CH/ π interactions in a pair of molecules of **7b** between a CF₃–phenyl group and a methylene C–H group of the lactam rings were observed. The aniline NH group in **7b** formed an intermolecular hydrogen bond with a lactam carbonyl oxygen. A pair of intermolecular hydrogen bonds between the lactam amides as observed in biphenyl **4** and carbazole **6a** were observed. The total energy of the crystal packing of **7b** was found to be the lowest [−53.7 kcal/mol (vdW, −29.7 kcal/mol; electrostatic, −24.0 kcal/mol)] among three KSP inhibitors (Table 2).

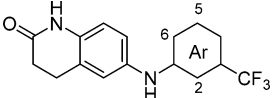
Taken together, the packing modes of the crystals of the three KSP inhibitors were revealed by X-ray crystal structure analysis. All crystal structures share common intermolecular hydrogen bonds across the lactam amide groups of two

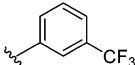
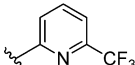
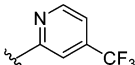
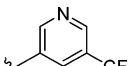
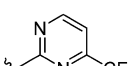
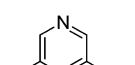
molecules to affect the crystal packings (Figure 3B,D,F). The total energies of the crystal packings correlated with the order of the melting points. For example, the higher total packing energy may rationalize the higher melting point of carbazole **6a**. However, the thermodynamic solubility of a series of compounds was not estimated directly from the total energy of the crystal packing nor the melting points. The lower solubility of **4** could be explained by the high energy of the crystal packing from van der Waals interactions via a number of CH/ π and π – π interactions in the periodic lattice. Because electrostatic interactions, including intermolecular hydrogen bonds, in the crystals can be offset in aqueous solution by interactions with the surrounding solvent, the energy from electrostatic interactions may have less of an impact to the solubility. In the course of the calculation of the packing energies, the uncharged forms of three inhibitors were compared.²⁵ The hydrogen-bond acceptor nitrogen of the aniline moiety in diphenylamine **7b**, which is not involved in electrostatic interactions in the crystal, may have a favorable effect on solvation for the increased solubility. Indeed, the solubility of **7b** was much higher than that of carbazole **6a**, even though both molecules had similar packing energy values from van der Waals interactions.

Given the unique relevance of crystal packing to the solubility, further optimization from diphenylamine **7b** was attempted for novel KSP inhibitors with more potent bioactivity and favorable properties. Since the left-hand lactam-fused phenyl group plays a pivotal role in KSP

inhibition, replacement of the right-hand 3-CF₃-phenyl group with aromatic nitrogen heterocycles (**8a–e**) was examined (Table 3). 5-Pyridine **8c** and pyrazine derivatives **8e** with a

Table 3. KSP Inhibitory Activities and Thermodynamic Solubility of Diaryl Amines with a Right-Hand Aromatic Heterocycle



Ar	KSP ATPase IC ₅₀ (μM) ^{a,b}	solubility	
		50% EtOH ^c (mg/mL)	phosphate buffer (pH 7.4) (μg/mL)
	7b 0.045	1.80	<1
	8a 0.41	3.64	3.08
	8b 0.068	3.51	6.12
	8c 0.71	4.78	6.15
	8d 0.10	0.458	1.53
	8e 1.9	0.276	1.49

^aInhibition of microtubule-activated KSP ATPase activity. ^bIC₅₀ values were derived from the dose–response curves generated from triplicate data points. ^cSolubility in an equal volume of EtOH and 1/15 M phosphate buffer (pH 7.4).

nitrogen at the 5-position decreased the potency for KSP inhibition [IC₅₀(**8c**) = 0.71 μM; IC₅₀(**8e**) = 1.9 μM]. 2-Pyridine **8a** and pyrimidine derivatives **8d** also showed moderate inhibitory activity [IC₅₀(**8a**) = 0.41 μM; IC₅₀(**8d**) = 0.10 μM]. However, 6-pyridine **8b** retained the highly potent KSP inhibitory activity seen for the parent **7b** [IC₅₀(**8b**) = 0.068 μM].

The aqueous solubility of pyridine derivatives **8a–c** was significantly improved, as anticipated. Compound **8b** was approximately twice as soluble in 50% EtOH compared with **7b** and soluble even in phosphate buffer.^{26,27} In contrast, pyrimidine **8d** and pyrazine derivatives **8e** were less soluble in 50% EtOH and phosphate buffer compared with pyridine derivatives **8a–c**. This is partly because of the lower basicity of pyrimidine or pyrazine compared with that of pyridine. As such, compound **8b** was identified to be a novel KSP inhibitor with a favorable balance of potency and aqueous solubility. Compound **8b** exhibited a good inhibitory effect on cancer cell proliferation (see Supporting Information).

In conclusion, we have designed a new class of KSP inhibitors with a diaryl amine scaffold to improve aqueous solubility from carbazole-based KSP inhibitors. The kinetic analysis of KSP ATPase activity and molecular modeling study suggested that diphenylamine **7b** binds to the interface of α4 and α6 via van der Waals interactions and two hydrogen bonds, working as an ATP-competitive inhibitor. The diphenylamine **7b** showed four times greater solubility than the parent carbazoles **6a,b**. The investigations on the physicochemical properties and packing energy calculations of the crystals of a series of compounds revealed that the improvement in solubility of **7b** resulted from the reduction in van der Waals interactions of CH/π and π–π, as well as increased solvation by a hydrogen-bond acceptor nitrogen of the aniline moiety. Further optimization of the right-hand CF₃-phenyl group in **7b** provided a potent and more soluble KSP inhibitor **8b** with a pyridinylamine moiety.

■ ASSOCIATED CONTENT

Supporting Information

Experimental procedures, characterization, bioassay data, and crystallographic information. This material is available free of charge via the Internet at <http://pubs.acs.org>.

■ AUTHOR INFORMATION

Corresponding Authors

*(S.O.) Tel: +81-75-753-4551. Fax: +81-75-753-4570. E-mail: soishi@pharm.kyoto-u.ac.jp.

*(N.F.) E-mail: nfujii@pharm.kyoto-u.ac.jp.

Funding

This work was supported by Grants-in-Aid for Scientific Research; and Platform for Drug Discovery, Informatics, and Structural Life Science from MEXT, Japan. T.T. is grateful for JSPS Research Fellowships for Young Scientists.

Notes

The authors declare no competing financial interest.

■ ACKNOWLEDGMENTS

We thank Dr. Mikio Yamasaki and Dr. Takashi Matsumoto (Rigaku Corporation) for their supports for X-ray analysis.

■ ABBREVIATIONS

KSP, kinesin spindle protein; CENP-E, centromere-associated protein E; MKLP-1, mitotic kinesin-like protein 1

■ REFERENCES

- (1) Rath, O.; Kozielski, F. Kinesins and cancer. *Nat. Rev. Cancer* **2012**, *12*, 527–539.
- (2) Mayer, T. U.; Kapoor, T. M.; Haggarty, S. J.; King, R. W.; Schreiber, S. L.; Mitchison, T. J. Small molecule inhibitor of mitotic spindle bipolarity identified in a phenotype-based screen. *Science* **1999**, *286*, 971–974.
- (3) Sakowicz, R.; Finer, J. T.; Beraud, C.; Crompton, A.; Lewis, E.; Fritsch, A.; Lee, Y.; Mak, J.; Moody, R.; Turincio, R.; Chabala, J. C.; Gonzales, P.; Roth, S.; Weitman, S.; Wood, K. W. Antitumor activity of a kinesin inhibitor. *Cancer Res.* **2004**, *64*, 3276–3280.
- (4) Jackson, J. R.; Patrick, D. R.; Dar, M. M.; Huang, P. S. Targeted anti-mitotic therapies: can we improve on tubulin agents? *Nat. Rev. Cancer* **2007**, *7*, 107–117.
- (5) Matsuno, K.; Sawada, J.; Asai, A. Therapeutic potential of mitotic kinesin inhibitors in cancer. *Expert Opin. Ther. Pat.* **2008**, *18*, 253–274.

- (6) Sarli, V.; Giannis, A. Targeting the kinesin spindle protein: basic principles and clinical implications. *Clin. Cancer Res.* **2008**, *14*, 7583–7587.
- (7) Oishi, S.; Watanabe, T.; Sawada, J.; Asai, A.; Ohno, H.; Fujii, N. Kinesin spindle protein (KSP) inhibitors with 2,3-fused indole scaffolds. *J. Med. Chem.* **2010**, *53*, 5054–5058.
- (8) Nakazawa, J.; Yajima, J.; Usui, T.; Ueki, M.; Takatsuki, A.; Imoto, M.; Toyoshima, Y.; Osada, H. A novel action of terpendole E on the motor activity of mitotic Kinesin Eg5. *Chem. Biol.* **2003**, *10*, 131–137.
- (9) Hotha, S.; Yarrow, J. C.; Yang, J. G.; Garrett, S.; Renduchintala, K. V.; Mayer, T. U.; Kapoor, T. M. HR22C16: a potent small-molecule probe for the dynamics of cell division. *Angew. Chem., Int. Ed.* **2003**, *42*, 2379–2382.
- (10) Parrish, C. A.; Adams, N. D.; Auger, K. R.; Burgess, J. L.; Carson, J. D.; Chaudhari, A. M.; Copeland, R. A.; Diamond, M. A.; Donatelli, C. A.; Duffy, K. J.; Faucette, L. F.; Finer, J. T.; Huffman, W. F.; Hugger, E. D.; Jackson, J. R.; Knight, S. D.; Luo, L.; Moore, M. L.; Newlander, K. A.; Ridgers, L. H.; Sakowicz, R.; Shaw, A. N.; Sung, C. M. M.; Sutton, D.; Wood, K. W.; Zhang, S. Y.; Zimmerman, M. N.; Dhanak, D. Novel ATP-competitive kinesin spindle protein inhibitors. *J. Med. Chem.* **2007**, *50*, 4939–4952.
- (11) Luo, L.; Parrish, C. A.; Nevins, N.; McNulty, D. E.; Chaudhari, A. M.; Carson, J. D.; Sudakin, V.; Shaw, A. N.; Lehr, R.; Zhao, H.; Sweitzer, S.; Lad, L.; Wood, K. W.; Sakowicz, R.; Annan, R. S.; Huang, P. S.; Jackson, J. R.; Dhanak, D.; Copeland, R. A.; Auger, K. R. ATP-competitive inhibitors of the mitotic kinesin KSP that function via an allosteric mechanism. *Nat. Chem. Biol.* **2007**, *3*, 722–726.
- (12) Matsuno, K.; Sawada, J.; Sugimoto, M.; Ogo, N.; Asai, A. Bis(hetero)aryl derivatives as unique kinesin spindle protein inhibitors. *Bioorg. Med. Chem. Lett.* **2009**, *19*, 1058–1061.
- (13) Takeuchi, T.; Oishi, S.; Watanabe, T.; Ohno, H.; Sawada, J.; Matsuno, K.; Asai, A.; Asada, N.; Kitaura, K.; Fujii, N. Structure–activity relationships of carboline and carbazole derivatives as a novel class of ATP-competitive kinesin spindle protein inhibitors. *J. Med. Chem.* **2011**, *54*, 4839–4846.
- (14) Ding, S.; Nishizawa, K.; Kobayashi, T.; Oishi, S.; Lv, J.; Fujii, N.; Ogawa, O.; Nishiyama, H. A potent chemotherapeutic strategy for bladder cancer: (*S*)-methoxy-trityl-L-cystein, a novel Eg5 inhibitor. *J. Urol.* **2010**, *184*, 1175–1181.
- (15) Xing, N. D.; Ding, S. T.; Saito, R.; Nishizawa, K.; Kobayashi, T.; Inoue, T.; Oishi, S.; Fujii, N.; Lv, J. J.; Ogawa, O.; Nishiyama, H. A potent chemotherapeutic strategy in prostate cancer: *S*-(methoxy-trityl)-L-cystein, a novel Eg5 inhibitor. *Asian J. Androl.* **2011**, *13*, 236–241.
- (16) For a recent review, see: Ishikawa, M.; Hashimoto, Y. Improvement in aqueous solubility in small molecule drug discovery programs by disruption of molecular planarity and symmetry. *J. Med. Chem.* **2011**, *54*, 1539–1554.
- (17) Anderson, K. W.; Tundel, R. E.; Ikawa, T.; Altman, R. A.; Buchwald, S. L. Monodentate phosphines provide highly active catalysts for Pd-catalyzed C–N bond-forming reactions of hetero-aromatic halides/amines and (H)N-heterocycles. *Angew. Chem., Int. Ed.* **2006**, *45*, 6523–6527.
- (18) Song, Y.; Wang, J.; Teng, S. F.; Kesuma, D.; Deng, Y.; Duan, J.; Wang, J. H.; Qi, R. Z.; Sim, M. M. β -Carbolines as specific inhibitors of cyclin-dependent kinases. *Bioorg. Med. Chem. Lett.* **2002**, *12*, 1129–1132.
- (19) Garcia-Saez, I.; Yen, T.; Wade, R. H.; Kozielski, F. Crystal structure of the motor domain of the human kinetochore protein CENP-E. *J. Mol. Biol.* **2004**, *340*, 1107–1116.
- (20) Avdeef, A.; Testa, B. Physicochemical profiling in drug research: a brief survey of the state-of-the-art of experimental techniques. *Cell. Mol. Life Sci.* **2002**, *59*, 1681–1689.
- (21) The compounds **4**, **6a,b**, and **7b** were insoluble in phosphate buffer (pH 7.4) (<1 $\mu\text{g/mL}$).
- (22) Jain, N.; Yalkowsky, S. H. Estimation of the aqueous solubility I: application to organic nonelectrolytes. *J. Pharm. Sci.* **2001**, *90*, 234–252.
- (23) Scott, J. S.; Birch, A. M.; Brocklehurst, K. J.; Broo, A.; Brown, H. S.; Butlin, R. J.; Clarke, D. S.; Davidsson, Ö.; Ertan, A.; Goldberg, K.; Groombridge, S. D.; Hudson, J. A.; Laber, D.; Leach, A. G.; MacFaul, P. A.; McKerrecher, D.; Pickup, A.; Schofield, P.; Svensson, P. H.; Sorme, P.; Teague, J. Use of small-molecule crystal structures to address solubility in a novel series of G protein coupled receptor 119 agonists: optimization of a lead and in vivo evaluation. *J. Med. Chem.* **2012**, *55*, 5361–5379.
- (24) The single crystals of carbazole **6a** were easily collapsed to give amorphous powder. The solubility of this single crystal was identical (0.423 mg/mL in 50% EtOH) to that of the powder form.
- (25) The charged form of diphenylamine **7b** in solution was not considered because the pK_a value of protonated diphenylamine was reported to be 0.78; see Dolman, D.; Stewart, R. An acidity function in ethanol-sulfuric acid based on the protonation of diphenylamines. *Can. J. Chem.* **1967**, *45*, 903–910.
- (26) The charged pyridine form of **8b** in solution was not considered because of the reported pK_a value (5.40) of protonated 2-(*N*-phenylamino)pyridine; see Weisstuch, A.; Testa, A. C. Fluorescence study of 2-(*N,N*-dimethylamino)pyridine and related molecules. *J. Phys. Chem.* **1970**, *74*, 2299–2303.
- (27) Although diaryl amine **8b** is much more soluble compared with the parent carbazole **6a**, further optimization may be needed.